J. Fluid Mech. (2000), *vol.* 406, *pp.* 337–346. Printed in the United Kingdom

© 2000 Cambridge University Press

A note on the instabilities of a horizontal shear flow with a free surface

By L. ENGEVIK

Department of Mathematics, University of Bergen, N-5020, Norway

(Received 22 June 1999 and in revised form 16 November 1999)

The instabilities of a free surface shear flow are considered, with special emphasis on the shear flow with the velocity profile $U^\star = U_0^\star \mathrm{sech}^2(by^\star)$. This velocity profile, which is found to model very well the shear flow in the wake of a hydrofoil, has been focused on in previous studies, for instance by Dimas & Triantyfallou who made a purely numerical investigation of this problem, and by Longuet-Higgins who simplified the problem by approximating the velocity profile with a piecewise-linear profile to make it amenable to an analytical treatment. However, none has so far recognized that this problem in fact has a very simple solution which can be found analytically; that is, the stability boundaries, i.e. the boundaries between the stable and the unstable regions in the wavenumber (k)–Froude number (F)-plane, are given by simple algebraic equations in k and F. This applies also when surface tension is included. With no surface tension present there exist two distinct regimes of unstable waves for all values of the Froude number $F > 0$. If $0 < F \ll 1$, then one of the regimes is given by $0 < k < (1 - F^2/6)$, the other by $F^{-2} < k < 9F^{-2}$, which is a very extended region on the k-axis. When $F \gg 1$ there is one small unstable region close to $k = 0$, i.e. $0 < k < 9/(4F^2)$, the other unstable region being $(3/2)^{1/2}F^{-1} < k < 2 + 27/(8F^2)$. When surface tension is included there may be one, two or even three distinct regimes of unstable modes depending on the value of the Froude number. For small F there is only one instability region, for intermediate values of F there are two regimes of unstable modes, and when F is large enough there are three distinct instability regions.

1. Introduction

The instabilities of a horizontal shear flow with a free surface are considered. While the stability of shear flows in unbounded fluids has been widely studied, both linearly and nonlinearly (see Maslowe 1981), the stability of a shear flow with a free surface has received less attention and is less well understood. In a recent paper Longuet-Higgins (1998) introduced a shear-flow model with a piecewise-linear velocity profile to replace the original one in order to simplify the stability analysis. This idea was applied to the shear flow with the velocity profile,

$$U^\star = U_0^\star \mathrm{sech}^2(by^\star), \tag{1.1}$$

the stability of which had previously been studied numerically by Triantafyllou & Dimas (1989) and Dimas & Triantafyllou (1994), who adopted this profile to fit experimental data of the shear flow in a wake of a hydrofoil. Instead of using this elaborate numerical method of calculation Longuet-Higgins proposed to approximate the velocity profile (1.1) by a piecewise-linear profile and found that then the solution of the stability problem was reduced to determining the roots of a quartic polynomial.

https://doi.org/10.1017/S0022112099007612 Published online by Cambridge University Press

However, it turns out that the stability problem with the velocity profile (1.1) has a very simple solution which can be found analytically. To be precise, the stability boundaries in the wavenumber (k)–Froude number (F)-plane are given by simple algebraic equations in k and F. In this note the effect of the surface tension is also considered.

The plan of the paper is as follows. Section 2 introduces the basic equations and some general results concerning the stability of a shear flow with a free surface. In § 3 the shear flow with the velocity profile (1.1) is discussed both with and without surface tension. The stability boundaries for the piecewise-linear velocity profile used by Longuet-Higgins to approximate the profile (1.1) are calculated in § 4, and a comparison with the results for the profile (1.1) is made.

2. Mathematical formulation

The basic flow velocity $\boldsymbol{v}_b$ is assumed to be directed along the $x^\star$-axis and varies in the vertical direction which is the $y^\star$-direction, i.e. $\boldsymbol{v}_b = U^\star(y^\star)\boldsymbol{i}$, where $\boldsymbol{i}$ is the unit vector in the $x^\star$-direction. The fluid is assumed to be homogeneous, incompressible and inviscid. In this note we will consider only perturbations of the normal mode type and then, since Squire's transformation holds with a rescaling of the physical parameters (Yih 1955), only the two-dimensional stability problem need be solved. It is well known that three-dimensional perturbations which are not of the normal mode type, and which show an algebraic growth with time, do occur in shear flows confined between rigid walls (Ellingsen & Palm 1975). Such perturbations are most probably also present in the free surface shear flow problem, but are beyond the scope of this note.

Since we consider only two-dimensional perturbations a streamfunction $\psi^\star(x^\star,y^\star,t^\star)$ can be introduced. The linearized equation for the streamfunction is

$$\left(\frac{\partial}{\partial t^\star} + U^\star\frac{\partial}{\partial x^\star}\right)\nabla^2\psi^\star - U^{\star\prime\prime}\frac{\partial\psi^\star}{\partial x^\star} = 0. \tag{2.1}$$

This equation is subjected to the dynamic and the kinematic boundary condition at the free surface $y^\star = \zeta^\star(x^\star,t^\star)$. The linearized boundary conditions at the free surface are

$$\left.\begin{aligned}\left(\frac{\partial}{\partial t^\star} + U^\star\frac{\partial}{\partial x^\star}\right)u + U^{\star\prime}v &= -g\frac{\partial\zeta^\star}{\partial x^\star} + \frac{\tau}{\rho}\frac{\partial^3\zeta^\star}{\partial x^{\star 3}}\\ v &= \left(\frac{\partial}{\partial t^\star} + U^\star\frac{\partial}{\partial x^\star}\right)\zeta^\star\end{aligned}\right\} \quad \text{at } y^\star = 0, \tag{2.2}$$

where $u = \partial\psi^\star/\partial y^\star$ and $v = -\partial\psi^\star/\partial x^\star$ are the perturbation velocity components in the $x^\star$- and the $y^\star$-directions, g is the acceleration due to gravity, ρ the density and τ the surface tension. Prime denotes differentiation with respect to $y^\star$. Also,

$$\psi^\star(x^\star,y^\star,t^\star) \to 0 \quad \text{when } y^\star \to -\infty. \tag{2.3}$$

These equations are made dimensionless by introducing the velocity scale $U_0^\star = U^\star(0)$, the length scale H, which is a characteristic length for the variation of $U^\star(y^\star)$ with depth, and the time scale $H/U_0^\star$. In the following we work with dimensionless quantities and U, $\psi(x,y,t)$, x, y and t denote the shear flow velocity, the steamfunction, the coordinates and the time respectively.

https://doi.org/10.1017/S0022112099007612 Published online by Cambridge University Press

We consider a wave solution of the form

$$\psi(x, y, t) = \phi(y) \exp\{ik(x - ct)\}, \tag{2.4}$$

where $\phi(y)$ is the amplitude function, k the wavenumber and c the wave velocity. Equation (2.4) is introduced into the dimensionless version of (2.1), (2.2) and (2.3) to obtain the equations which ϕ has to satisfy,

$$(U(y) - c)(\phi'' - k^2\phi) - U''(y)\phi = 0, \quad -\infty < y < 0, \tag{2.5}$$

$$(1 - c)^2\phi' = \left[U'(0)(1 - c) + F^{-2}(1 + Tk^2)\right]\phi \quad \text{at } y = 0, \tag{2.6}$$

$$\phi \to 0 \quad \text{when } y \to -\infty, \tag{2.7}$$

where $F = U_0^\star/(gH)^{1/2}$ is the Froude number and $T = \tau/(\rho g H^2)$.

Equation (2.5) is the Rayleigh equation. Equation (2.6) is obtained from the dynamic and the kinematic boundary condition at $y = 0$ as given by (2.2). Equations (2.5)–(2.7) may have neutral solutions which form the stability boundaries in the (k, F)-plane. Let ϕ_s, k_s and c_s denote the amplitude function, the wavenumber and the wave velocity of a neutral solution. Yih (1972) showed that if $U(y)$ is a monotonic function of y and $U_{min} < c_s < U_{max}$ then $c_s = U(y_s)$, where y_s is an inflection point of $U(y)$. Yih's proof, however, does not exclude possible neutral solutions with wave velocities $c_s = U_{min}$ and $c_s = U_{max}$.

To determine on what side of the neutral curve in the (k, F)-plane there is instability we have to know the stability characteristics in the neighbourhood of the curve, which can be achieved by a perturbation of the known neutral solution. Suppose that there exists an unstable solution near the neutral one and that the wave velocity can be expanded in a series in powers of $(k - k_s)$, i.e.

$$c - c_s = c_1(k - k_s) + \cdots, \tag{2.8}$$

where $c_1 = c_{1r} + \mathrm{i}c_{1i}$ is a constant.

Both the unstable and the neutral solution satisfy (2.5)–(2.7), from which it follows that

$$\phi_s(0)\phi'(0) - \phi_s'(0)\phi(0) - (c - c_s)\int_{-\infty}^{0} \frac{U''\phi_s\phi}{(U - c_s)(U - c)}\,\mathrm{d}y - (k^2 - k_s^2)\int_{-\infty}^{0} \phi_s\phi\,\mathrm{d}y = 0. \tag{2.9}$$

The first two terms are the contribution from the free surface condition at $y = 0$. If $F = 0$ this contribution is equal to zero. If we let $F \neq 0$ and introduce (2.8) into (2.9) we find that c_1 must satisfy the equation

$$\left[\frac{U'(0)\phi_s^2(0)}{(1 - c_s)^2} + \frac{2(1 + Tk_s^2)\phi_s^2(0)}{F^2(1 - c_s)^3} - \lim_{c \to c_s}\int_{-\infty}^{0} \frac{U''\phi_s^2}{(U - c_s)(U - c)}\,\mathrm{d}y\right] c_1 - 2k_s\left[\int_{-\infty}^{0} \phi_s^2\,\mathrm{d}y - \frac{T\phi_s^2(0)}{F^2(1 - c_s)^2}\right] = 0. \tag{2.10}$$

This expression for c_1 can be used to determine on what side of the neutral curve there is instability. Let $U(y)$ be a monotonic function of y and let $U(-\infty) = 0$. Then $U_{min} = 0$ and $U_{max} = U(0) = 1$. If $U(y)$ has an inflection point at y_s, where

https://doi.org/10.1017/S0022112099007612 Published online by Cambridge University Press

$-\infty < y_s < 0$, and there exists a neutral solution with $c_s = U(y_s)$ then

$$c_1 = 2k_s \left[\int_{-\infty}^{0} \phi_s^2 \, \mathrm{d}y - \frac{T\phi_s^2(0)}{F^2(1-c_s)^2} \right] \left(\frac{R - \mathrm{i}I}{R^2 + I^2} \right), \tag{2.11}$$

where

$$R = \frac{U'(0)\phi_s^2(0)}{(1-c_s)^2} + \frac{2(1+Tk_s^2)\phi_s^2(0)}{F^2(1-c_s)^3} - P\int_{-\infty}^{0} \frac{U''\phi_s^2}{(U-c_s)^2}\mathrm{d}y,$$

$$I = -\pi \frac{U'''(y_s)\phi_s^2(y_s)}{(U'(y_s))^2}.$$

P in front of the integral sign means the principal value of the integral. When the integral in the coefficient of c_1 in (2.10) is evaluated Plemelj's formula (see Muskhelishvili 1953) has been used. On the instability side of the neutral curve $c_i = c_{1i}(k - k_s) > 0$, which together with the expression for c_{1i} given by (2.11) yields the instability side.

If there exist neutral solutions with $c_s = U_{min} = 0$ and $c_s = U_{max} = 1$ then c_1 given by (2.10) is real if it exists, which means that c_i is of a higher order in $(k - k_s)$ than c_r is. Then, in order to determine the instability side of the neutral curve the expression for c_1 can be used together with Howard's semicircle theorem, which was shown by Yih (1972) to be applicable also for shear flows with a free surface. This is demonstrated for the velocity profile (1.1).

3. The velocity profile $U^\star = U_0^\star \mathrm{sech}^2(by^\star)$

The dimensionless version of this velocity profile, which is to be introduced into (2.5)–(2.7), is $U(y) = \mathrm{sech}^2(y)$, where we have taken the length scale H to be b^{-1}. We introduce the new variable $\eta = \tanh(y)$ into (2.5)–(2.7) and obtain

$$(1-\eta^2-c)\left\{(1-\eta^2)\phi'' - 2\eta\phi' - \frac{k^2}{1-\eta^2}\phi\right\} - (6\eta^2 - 2)\phi = 0, \quad -1 < \eta < 0, \tag{3.1}$$

$$(1-c)^2\phi' = F^{-2}(1+Tk^2)\phi \quad \text{at } \eta = 0, \tag{3.2}$$

$$\phi = 0 \quad \text{at } \eta = -1, \tag{3.3}$$

where the prime now denotes the differentiation with respect to η.

We have the following three options for neutral solutions: $c_s = U(\eta_s) = \frac{2}{3}$, where η_s is the inflection point of the velocity profile, $c_s = 0$ and $c_s = 1$. If we put $c_s = \frac{2}{3}$ and $c_s = 0$ into (3.1) we find that in both cases we have to solve the following equation to find the neutral solution ϕ_s:

$$(1-\eta^2)\phi'' - 2\eta\phi' + \left(6 - \frac{m^2}{1-\eta^2}\right)\phi = 0, \tag{3.4}$$

where $m^2 = k^2$ when $c_s = \frac{2}{3}$ and $m^2 = 4 + k^2$ when $c_s = 0$.

For $m = 0$ this is the Legendre equation with the solution $P_2(\eta)$, the Legendre polynomial of degree two, which is finite at $\eta = -1$. For $m \neq 0$ this is the associated Legendre equation, which, when $m = 1$ and $m = 2$, has the solutions $P_2^1(\eta)$ and $P_2^2(\eta)$, the associated Legendre functions of the first kind, which are finite at $\eta = -1$. These solutions, however, satisfy the boundary condition at $\eta = 0$ only in the extreme cases, $F = 0$ ($\phi_s = P_2^1$) and $F = \infty$ ($\phi_s = P_2$ and $\phi_s = P_2^2$). However, it can be shown that

https://doi.org/10.1017/S0022112099007612 Published online by Cambridge University Press

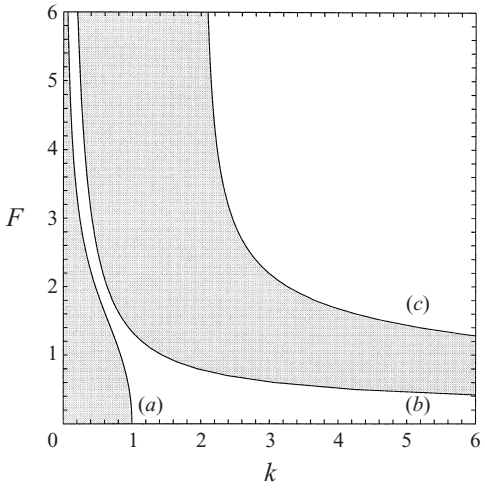


FIGURE 1. Stability diagram for the velocity profile $U = \mathrm{sech}^2(y)$. No surface tension, i.e. $T = 0$. The shaded regions are the unstable regions. The curves (a) and (c) are the loci of the neutral solutions with velocity $c_s = \frac{2}{3}$, and the curve (b) the locus of the neutral solutions with $c_s = 0$.

(3.4) has a simple closed-form solution for all values of $m \geqslant 0$, satisfying the boundary condition at $\eta = -1$, i.e.

$$\phi_s(\eta) = \left(\frac{1+\eta}{1-\eta}\right)^{m/2} \left(3\eta^2 - 3m\eta + m^2 - 1\right). \tag{3.5}$$

(We see that $\phi_s(-1)$ is finite but not zero when $m = 0$; $\phi_s(-1) = 2P_2(-1)$.)

We will consider the two cases, $T = 0$ (no surface tension), and $T \neq 0$ (surface tension present).

(i) $T = 0$

If we put $c = c_s = \frac{2}{3}$ or $c = c_s = 0$ and ϕ_s given by (3.5) into (3.2) we find that m has to satisfy the equation

$$m^3 - 4m = \frac{\alpha}{F^2}(m^2 - 1), \tag{3.6}$$

where $\alpha = 9$ when $c_s = \frac{2}{3}$, and $\alpha = 1$ when $c_s = 0$.

The solutions of (3.6) can be considered as the intersections between the graphs of the polynomials on the left-hand side and on the right-hand side of (3.6) respectively, which clearly shows that (3.6) has one solution $m_{1(\alpha)} \leqslant 1$ and one $m_{2(\alpha)} \geqslant 2$. (We are only interested in the solutions where $m \geqslant 0$.) This yields two neutral solutions with wave velocity $c_s = \frac{2}{3}$: one with wavenumber $k_s = m_{1(9)}$ and one with wavenumber $k_s = m_{2(9)}$. However, there is only one neutral solution with wave velocity $c_s = 0$ and wavenumber $k_s = (m_{2(1)}^2 - 4)^{1/2}$.

When $F = 0$ there is only one solution $m_{1(\alpha)} = 1$ of (3.6) which yields the neutral solution with $c_s = \frac{2}{3}$ and $k_s = 1$, and no neutral solution with $c_s = 0$. When $F = \infty$ then $m_{1(\alpha)} = 0$ and $m_{2(\alpha)} = 2$, and there are two neutral solutions with $c_s = \frac{2}{3}$ – one with $k_s = 0$ and one with $k_s = 2$ – and one neutral solution with $c_s = 0$ and $k_s = 0$.

In terms of the wavenumber we get the following equations to be solved when $c_s = \frac{2}{3}$ and when $c_s = 0$:

$$F^2k^3 - 9k^2 - 4F^2k + 9 = 0, \tag{3.7}$$

https://doi.org/10.1017/S0022112099007612 Published online by Cambridge University Press

$$F^2k^2\sqrt{k^2+4}-k^2-3=0. \tag{3.8}$$

The solutions of (3.7) and (3.8) are plotted in figure 1, giving the stability boundaries in the (k,F)-plane: two curves, labelled (a) and (c), on which $c_s=\frac{2}{3}$ and one, labelled (b), on which $c_s=0$. Since $U'''(\eta_s)<0$ (2.11) shows that $c_{1i}<0$ and then there is instability to the left of the neutral curves (a) and (c). When $c_s=0$ numerical calculations show that c_{1r} given by (2.10) is greater than zero, which together with the semicircle theorem yields that there is instability to the right of the neutral curve (b).

In addition to these neutral solutions there is one with $c_s=1$ and $k_s=0$ as well; the amplitude function being $\phi_s=\eta^2$. This solution is valid for all F. Both $\phi_s(0)=0$ and $\phi_s'(0)=0$ so the contribution from the surface condition at $y=0$ in (2.9) is equal to zero in this case. However, the integrals in (2.10) do not exist so this formula for c_1 is not applicable in this case. However, close to this neutral solution there exists an unstable solution which is found to be

$$\phi(\eta)=(1-\eta^2)^{k/2}[\eta^2-\tilde{c}+k\theta(\eta)+\cdots], \tag{3.9}$$

where $c=1-\tilde{c}$, $k\ll 1$ and $|\tilde{c}|\ll 1$. We find that $\tilde{c}=\tilde{c}_r+\mathrm{i}\tilde{c}_i=(k\pi/4)^{2/3}(\frac{1}{2}-\mathrm{i}\frac{1}{2}\sqrt{3})$, which shows why the expression for c_1 given by (2.10) does not apply in this case; our assumption expressed by (2.8) is simply not valid. $\theta(\eta)$ is easily found, but the expression is lengthy and will not be given here. Notice that the solution given by (3.9) satisfies the boundary condition at $\eta=-1$, which the neutral solution does not; $\phi(\eta)$ given by (3.9) lies close to $\phi_s=\eta^2$ for all $\eta\neq -1$.

The above analysis shows that there are two distinct regimes of unstable modes for a given Froude number, previously referred to as Branch I and Branch II by Triantyfallou & Dimas (1989): Branch I at low wavenumbers and Branch II at higher wavenumbers. Branch I and Branch II are separated for all values of the Froude number; they never merge. Branch I is bounded to the left by $k=0$ and to the right by $k=m_{1(9)}$, and Branch II is bounded to the left and to the right by $k=(m_{2(1)}^2-4)^{1/2}$ and $k=m_{2(9)}$ respectively. When $F=0$ only Branch I is present. When $0<F\ll 1$ it follows from (3.7) and (3.8) that the wavenumbers of the Branch I modes and the Branch II modes lie in the regions $0<k<(1-F^2/6)$ and $F^{-2}<k<9F^{-2}$ respectively. When $F\gg 1$ we find that the Branch I region is $0<k<9/(4F^2)$ and the Branch II region is given by $(3/2)^{1/2}F^{-1}<k<2+27/(8F^2)$. We see that when F is increasing both regions shrink and in the end when $F=\infty$ then Branch I has shrunk to a point and only Branch II modes are left with wavenumbers in the region $0<k<2$.

(ii) $T\neq 0$

In this case we find that the wavenumbers of the neutral solutions with $c_s=\frac{2}{3}$ are given by the equation

$$9Tk^4-F^2k^3+9(1-T)k^2+4F^2k-9=0, \tag{3.10}$$

and the wavenumbers of the neutral solutions with $c_s=0$ by

$$Tk^4-F^2k^2\sqrt{k^2+4}+(1+3T)k^2+3=0. \tag{3.11}$$

Given T, (3.10) and (3.11) yield the stability boundaries in the (k,F)-plane: two curves, labelled (a) and (c), on which $c_s=\frac{2}{3}$ and one, labelled (b), on which $c_s=0$. For $T=0.5$ these stability boundaries are plotted in figure 2. The neutral curve (b) has a minimum at $k=k_1=2.035$ and $F=F_1=1.362$, and the neutral curve (c) a minimum at $k=k_2=3.59$ and $F=F_2=4.996$. Comparing figure 1 and figure 2 shows that the surface tension has little influence on the Branch I, but it affects the

https://doi.org/10.1017/S0022112099007612 Published online by Cambridge University Press

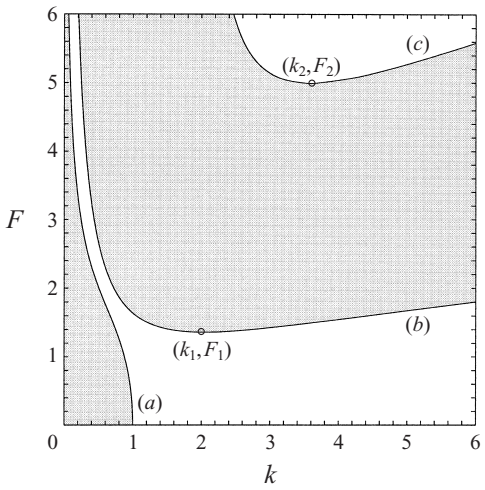


FIGURE 2. Stability diagram for the velocity profile $U = \mathrm{sech}^2(y)$. Surface tension present, $T = 0.5$. The shaded regions are the unstable regions. The curves (a) and (c) are the loci of the neutral solutions with velocity $c_s = \frac{2}{3}$, and the curve (b) the locus of the neutral solutions with $c_s = 0$. The points (k_1, F_1) and (k_2, F_2) are the minimum points of the curves (b) and (c) respectively.

Branch II considerably. We see that when $F < F_1$ there are no Branch II modes so the surface tension has stabilized these unstable modes which are present when $T = 0$. Only Branch I modes exist when $F < F_1$. When $F_1 < F < F_2$ there are again two distinct regimes of unstable modes. Now the Branch II region is bounded by a neutral solution with $c_s = 0$ both to the right and to the left. For a given $F > F_2$ there are three separated instability regions on the k-axis, a small Branch I region close to $k = 0$, a Branch II region bounded by the neutral solution with $c_s = 0$ to the left and the neutral solution with $c_s = \frac{2}{3}$ to the right, and a Branch III region bounded by the neutral solutions with $c_s = \frac{2}{3}$ and with $c_s = 0$ to the left and to the right respectively. Applying the perturbation formulae (2.10) and (2.11) yields instability on the shaded side of the neutral curves.

4. Comparison with the piecewise-linear profile

Longuet-Higgins approximated the velocity profile (1.1) by a piecewise-linear profile of the form

$$U^\star(y^\star) = \begin{cases} U_0^\star, & -H_1 < y^\star < 0 \\ \Omega(y^\star + H_2), & -H_2 < y^\star < -H_1 \\ 0, & y^\star < -H_2, \end{cases} \tag{4.1}$$

where $U_0^\star = \Omega(H_2 - H_1)$. The stability problem is then reduced to determining the roots of a quartic polynomial. If the following dimensionless quantities are introduced: $F = U_0^\star/(gH)^{1/2}$, $h_1 = H_1/H$, $h_2 = H_2/H$, $k = k^\star H$ and $c = c^\star/U_0^\star$, where $H = (H_1 + H_2)/2$, then this equation reads

$$a_4(c-1)^4 + a_3(c-1)^3 + a_2(c-1)^2 + a_1(c-1) + a_0 = 0, \tag{4.2}$$

$$a_0 = \left(Ak - \frac{A^2 B}{\lambda_1}\right)(\lambda_1 - 1),$$

https://doi.org/10.1017/S0022112099007612 Published online by Cambridge University Press

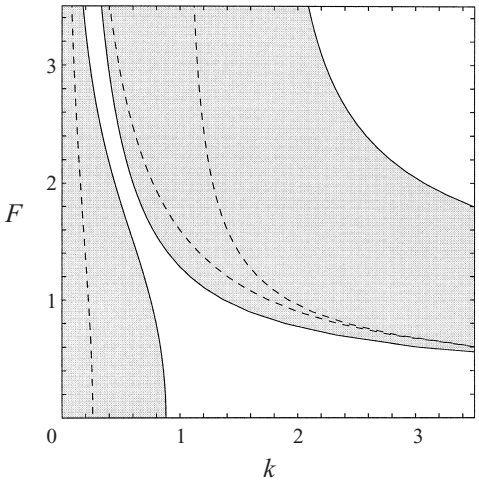


FIGURE 3. The shaded regions are the unstable regions for the velocity profile $U = \mathrm{sech}^2(y)$ with no surface tension present. The dashed lines are the stability boundaries for the piecewise-linear profile.

where

$$A = \frac{1}{2(h_2 - h_1)}, \quad B = (\lambda_1 - \lambda_2), \quad \lambda_i = \exp(-2kh_i),$$

$$a_1 = (-k^2 + ABk), \quad a_2 = -k^2 + F^2 k \left(Ak - \frac{A^2 B}{\lambda_1} \right) (\lambda_1 + 1),$$

$$a_3 = F^2(k^3 + ABk^2), \quad a_4 = F^2 k^3.$$

To find the stability boundaries in the (k, F)-plane we have to solve (4.2) together with the equation

$$4a_4(c-1)^3 + 3a_3(c-1)^2 + 2a_2(c-1) + a_1 = 0. \tag{4.3}$$

Longuet-Higgins approximated the velocity profile (1.1) by taking $h_1 = 0.1977$ and the dimensionless $b = 0.8814$. The stability boundaries have been calculated for this piecewise-linear profile and are shown in figure 3. Also, the stability boundaries for the original profile (1.1) are shown in figure 3, where the difference in the length scale H used in this note (see § 3) and that used by Longuet-Higgins has been accounted for. We see that the piecewise-linear profile has much narrower bands of unstable modes than the original profile, which is especially emphasized at low Froude numbers.

Longuet-Higgins' method can be applied to many different smooth profiles, and the ratio H_1/H_2 in the piecewise-linear velocity model will vary according to the profile which it approximates; this ratio being 0.11 for the sech^2-profile. In addition to being flexible as demonstrated in the paper of Longuet-Higgins (1998) the method also provides an easy way to calculate the growth rates of the unstable modes of the piecewise-linear profile. However, it should be kept in mind that this model may give narrower bands of unstable modes than the original profile which was also noted by Morland, Saffman & Yuen (1991) for the case of the wind-induced drift current.

5. Conclusions

In this note it is shown that a complete picture of the regimes of unstable modes of the velocity profile (1.1), which models the current profile in the wake of hydrofoils,

https://doi.org/10.1017/S0022112099007612 Published online by Cambridge University Press

can be achieved very easily. It turns out that the neutral wave solutions which form the boundaries of the unstable regimes can be found analytically, and their wavenumbers are given by simple algebraic equations. In fact the stability boundaries are more easily obtained for this profile than for the piecewise-linear profile used by Longuet-Higgins to approximate the original one. If surface tension is absent there are two distinct regimes of unstable modes, Branch I and Branch II, for all Froude numbers not equal to zero. The inclusion of surface tension alters the picture considerably. Now there may be one, two or even three separated regimes of unstable modes for a given Froude number, depending on the value of the Froude number. For small Froude numbers only Branch I is left; the unstable Branch II modes, which are present when there is no surface tension, have now been stabilized by the surface tension. For intermediate Froude numbers there are two regions of unstable modes, Branch I and Branch II; the range of the wavenumbers of the unstable Branch II modes has been extended by the inclusion of the surface tension for almost all values of the Froude number. For large Froude numbers there are three distinct instability regimes, Branch I, Branch II and Branch III. It is found that for all Froude numbers the Branch I regime is little affected by a moderate surface tension T.

We notice that 'the principle of the exchange of stabilities' (i.e. $c = 0$ on the stability boundaries) is not valid for this profile. Such a transition to instability occurs only across one of the curves which form the stability boundaries.

The regimes of the unstable modes of the piecewise-linear profile, which was used by Longuet-Higgins to replace the original one, have also been calculated. It is found that these instability regions fit poorly with those of the original profile, especially the Branch II region at low Froude numbers. We also notice that while the wave velocity is constant along the curves which form the stability boundaries for the velocity profile (1.1) this is not so for the piecewise-linear profile.

The formula for c given in § 2 yields the stability characteristics near the neutral curves. To obtain detailed information on the unstable regimes away from the neutral curves the eigenvalue problem (2.5)–(2.7) has to be solved numerically. However, it may be of help to know the value of c near the neutral curve since it can be taken as the start value of c in a numerical iteration, as was done by Engevik, Haugan & Klemp (1985) where a similar problem was considered.

The velocity profile (1.1) is exceptional in the sense that the neutral solutions which form the stability boundaries can be found analytically, which is not true for most of the smooth velocity profiles. In the general case the stability problem has to be handled numerically.

The assistance of Mr T. Eldevik in making the figures is acknowledged.

REFERENCES

Dimas, A. A. & Triantyfallou, G. S. 1994 Nonlinear interaction of shear flow with a free surface. *J. Fluid Mech.* **260**, 211–246.

Ellingsen, T. & Palm, E. 1975 Stability of linear flow. *Phys. Fluids* **18**, 487–488.

Engevik, L., Haugan, P. M. & Klemp, S. 1985 Stability analysis adjacent to neutral solutions of the Taylor–Goldstein equation when Howard's formula breaks down. *J. Fluid Mech.* **159**, 347–358.

Longuet-Higgins, M. S. 1998 Instabilities of a horizontal shear flow with a free surface. *J. Fluid Mech.* **364**, 147–162.

Maslowe, S. A. 1981 Shear Flow Instabilities and Transition. *In Hydrodynamic Instabilities and Transition to Turbulence* (ed. H. L. Swinney & J. P. Gollub), vol. 45, pp. 181–228. Springer.

https://doi.org/10.1017/S0022112099007612 Published online by Cambridge University Press

Morland, L. C., Saffman, P. G. & Yuen, H. C. 1991 Waves generated by shear layer instabilities. *Proc. R. Soc. Lond.* A **433**, 441–450.

Muskhelishveli, N. I. 1953 *Singular Integral Equations.* Noordhoff.

Triantyfallou, G. S. & Dimas, A. A. 1989 Interaction of two-dimensional separated flows with a free surface at low Froude numbers. *Phys. Fluids* A **1**, 1813–1821.

Yih, C. S. 1955 Stability of two-dimensional parallel flows for three-dimensional disturbances. *Q. Appl. Maths* **12**, 434–435.

Yih, C. S. 1972 Surface waves in flowing water. *J. Fluid Mech.* **51**, 209–220.

https://doi.org/10.1017/S0022112099007612 Published online by Cambridge University Press